Effect of annealing on the contact resistance of Aluminum on a p-type substrate

Shrey Shah and George Patrick Watson[1, a)]
[1]Singh Center for Nanotechnology, University of Pennsylvania
3205 Walnut St. Philadelphia, PA 19104

(Dated: Received 1 September 2019; accepted 14 November 2019)

Aluminum contacts are widely used to form both ohmic and rectifying contacts. The process to form these contacts involves annealing, thus it is important to study the effect of annealing on the electrical properties of the contacts. Here, we present a way to measure the contact resistance of aluminum contacts formed on a p-type silicon substrate. It was found the contact resistivity decreased by an average of 18%. It was thus found that annealing at 400 °C in a forming gas environment improves the electrical properties of aluminum contacts.

Key Words: Metallization, Contact Resistance, Aluminum contacts, Contact resistivity

I. Introduction

Metal-semiconductor contacts have been widely investigated in the recent years due to the fact that these contacts affect the performance of electronic devices.[1] Among the metal-semiconductor contacts, Aluminum contacts are considered to be at the heart of metallization in silicon integrated circuits, as they are used both as ohmic contacts and as rectifying contacts.[2] It has also been reported that aluminum is uniquely suited as a single-element metallization system.[2] Aluminum is preferred because of its ease of processing, ability to reduce native silicon dioxide chemically and its low resistivity.[3] Usually the metallization scheme for aluminum includes depositing aluminum followed by annealing at 400-450°C. This annealing is done to promote adhesion and eliminate electrical damage associated with the metal deposition process.[4] In this paper we investigate the effect of annealing on the contact resistance and resistivity of Aluminum metal contacts on p-type Silicon substrate.

II. Theory

Contact resistance refers to the resistance associated with the metal-semiconductor barrier at the interface between the semiconductor and the metal contact.[5] The easiest technique to measure the contact resistance is the two-terminal contact resistance method.[6] For both the contacts on the top surface, the two terminal contact resistance method can be implemented as shown in Fig. 1. The equation to calculate the total resistance (R_t) using this method is given by Eq. (1)

$$R_t = 2R_c + 2R_{sp} + R_s + 2R_p \quad (1)$$

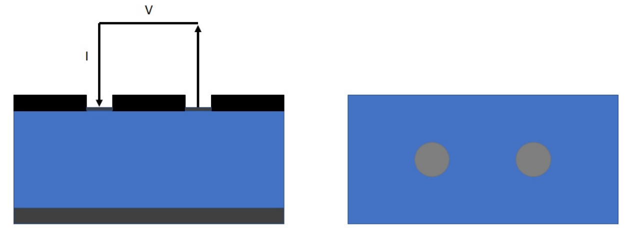

FIG. 1. Two-Terminal Contact Resistance Scheme

where R_c, R_{sp}, R_s and R_p are the contact resistance, spreading resistance, semiconductor resistance and probe resistance, respectively[3]. The semiconductor resistance R_s is usually negligible. The spreading resistance for the method we used and for small contacts can be approximated using Eq. (2).

$$R_s p = Cx(\rho/(4r)) \quad (2)$$

where ρ, C and r are semiconductor resistivity, correction factor and contact radius, respectively. For widely separated contacts and semi-infinite substrate the correction factor C has a value of 1.[3]

III. Experiment

Fig. 2 shows the process flow for making the device used for measuring contact resistance before and after annealing. For making the device, we started with a p-type silicon wafer on which silicon dioxide off approximately 280nm was grown thermally on both the sides. The silicon dioxide was stripped off from the back of the wafer using 1% hydrofluoric acid and a layer of aluminum of approximately 115 nm is sputtered at the back of the wafer for making a back contact. The fist level lithography is

a) Electronic mail: gewatson@seas.upenn.edu

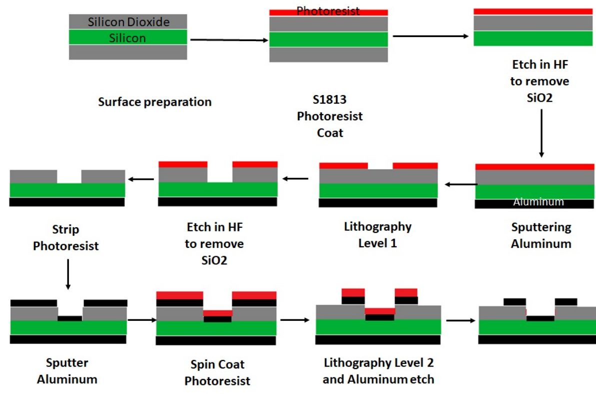

FIG. 2. Process sequence to manufacture device for measuring contact resistance

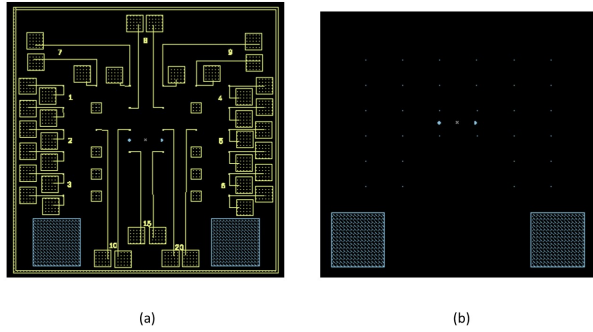

FIG. 3. (a) CAD layout of the entire device (b) CAD layout of circular aluminum contacts

performed using Heidelberg direct-write and then silicon dioxide was also etched from the exposed area as shown in Fig. 2. Later, aluminum of approximately 115nm is sputtered on the top of the wafer. The 2nd level lithography and stripping of Aluminum leads to the formation of the contacts for the device. The electrical measurements are taken before and after annealing at 400°C in forming gas(a mixture of hydrogen and nitrogen gas) for 15 minutes. Since it is important Since it is important for measuring the contact resistance accurately, we made small radius contacts ranging from 1μm to 9μm. The CAD file and the final device can be seen in Fig. 3 and Fig. 4, respectively.

IV. Results and Discussion

The bulk resistivity (ρ) of the device was measured using the four point probe method. The value of resistivity before and after annealing were 0.00314 Ωm and 0.00216 Ωm, respectively. It can be thus be seen that there is a 31% decrease in the resistivity upon annealing. The probe resistance was calculated by shorting the probes. The probe resistance R_p was found to be 1.714Ω. The total resistance R_t was measured using the scheme shown in Fig. 1 and the Voltage versus Current graph

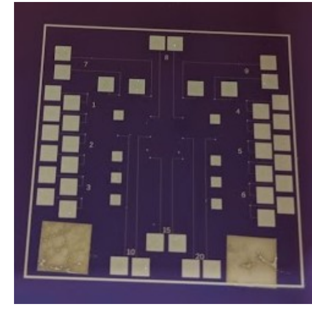

FIG. 4. 26mm x 26mm Contact resistance measurement device

TABLE I. Total resistance (R_t)before and after annealing

Radius (μm)	1	2	3	6
$R_{t,\ before}(\Omega)$	3091.7	2890.8	2839.1	2737
R_t(After)(Ω)	2408.9	2389.1	2274.9	2234.5
R_c(Before)(Ω)	1518.1	2102.3	2312.3	2471.9
R_c(After)(Ω)	1202.3	1784.1	1870.4	2030.5

from which the total resistance for each contact was measured are shown in Fig. 5. The total resistance for the contacts before and after annealing calculated from the Voltage versus Current graphs are shown in Table I.

After finding bulk resistivity (ρ),the spread resistance (R_{sp}),and probe resistance (R_p), the contact resistance was calculated using Eq. 1. Table I shows the contact resistance before and after annealing for contacts of different sizes. After annealing, the contact resistance decreases for all devices. The average percentage decrease in the contact resistance is around 14.8%. Table II shows the change in contact resistivity before and after annealing. The average contact resistivity decreased by 18%. The value of contact resistivity before and after annealing of 6.5x10^{-6} Ωcm^2 and 5.4x10^{-6} Ωcm^2 respectively are similar to that measured by Proctor *et al.* and Berger *et al.*[7,8]. The graph in Fig. 6 shows the difference in contact resistance upon annealing. The decrease in contact resistance is likely to be due to the aluminum intermixing with a native oxide on the surface of the silicon layer which leads to the formation of a more conductive interface. It may also be due to the fact that the annealing process helps promote adhesion and reduces any electrical damage caused during deposition. The apparent reduction in the bulk resistivity is not understood at this time. Some of the raw data and calculations can be found in Appendix A.

TABLE II. Contact resistivity before and after annealing

Radius (μm)	1	2	3	6
ρ_c(Before)(Ωcm^2)	4.8E-05	6.6E-05	7.3E-05	7.8E-05
ρ_c(After)(Ωcm^2)	3.8E-05	5.6E-05	5.9E-05	6.4E-05

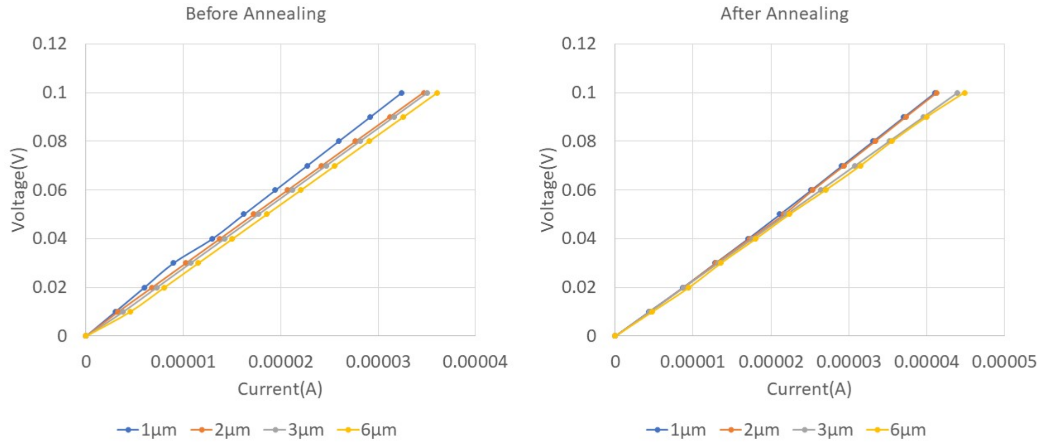

FIG. 5. Voltage versus current characteristics for contacts of radius 1μm,2μm,3μm and 6μm

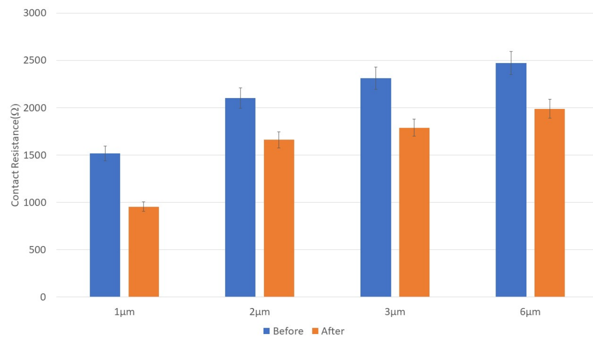

FIG. 6. Change of contact resistance after annealing in contacts with varied radius

V. Conclusion

This experiment found that after annealing at 400°C in forming gas for 15 min, which is the normally used annealing temperature and time for Aluminum contacts on Silicon, the contact resistance decreased by an average of 14.8%. This decrease in contact resistance leads to the formation of better Ohmic contacts and thus device performance. It was also found that the resistivity decreased by 31%. The average contact resistivity decreased by 18%. In conclusion, annealing leads to a reduction in both resistivity and contact resistance, thus leading to the formation of better electrical contacts.

VI. Acknowledgements

This work was performed at the Singh Center for Nanotechnology at the University of Pennsylvania, a member of the National Nanotechnology Coordinated Infrastructure (NNCI) network, which is supported by the National Science Foundation (Grant NNCI-1542153).

[1]M Siad, A Keffous, S Mamma, Y Belkacem, and H Menari. Correlation between series resistance and parameters of al/n-si and al/p-si schottky barrier diodes. *Applied surface science*, 236(1-4):366–376, 2004.
[2]Howard C Card. Aluminumsilicon schottky barriers and ohmic contacts in integrated circuits. *IEEE Transactions on Electron Devices*, 23(6):538–544, 1976.
[3]Dieter K Schroder. *Semiconductor material and device characterization*. John Wiley & Sons, 2015.
[4]S.M. Sze. *VLSI Technology*. Electronics and electronic circuits. McGraw-Hill, 1983.
[5]Daniel L Meier and Dieter K Schroder. Contact resistance: Its measurement and relative importance to power loss in a solar cell. *IEEE transactions on electron devices*, 31(5):647–653, 1984.
[6]Miles V Sullivan and John H Eigler. Five metal hydrides as alloying agents on silicon. *Journal of The Electrochemical Society*, 103(4):218–220, 1956.
[7]Stephen J Proctor, Loren W Linholm, and Jeffrey A Mazer. Direct measurements of interfacial contact resistance, end contact resistance, and interfacial contact layer uniformity. *IEEE Transactions on electron devices*, 30(11):1535–1542, 1983.
[8]HH Berger. Contact resistance and contact resistivity. *Journal of the Electrochemical Society*, 119(4):507–514, 1972.

A. Appendix A

The raw data of all the devices can be seen in Table III and IV. From these raw data, the contact resistance was calculated. The raw data used to calculate the probe resistance is shown in Table V.

The contact resistance was calculated using Eq. 1. The total resistance was found by plotting a linear trend-line for the data in Tables III and IV. For calculating the spreading resistance, the bulk resistivity was calculated using the four-point probe method. Finally, the probe resistance was calculated by plotting a trend-line for the data in Table V. By knowing the spread resistance, the total resistance and the probe resistance the contact resistance can be calculated.

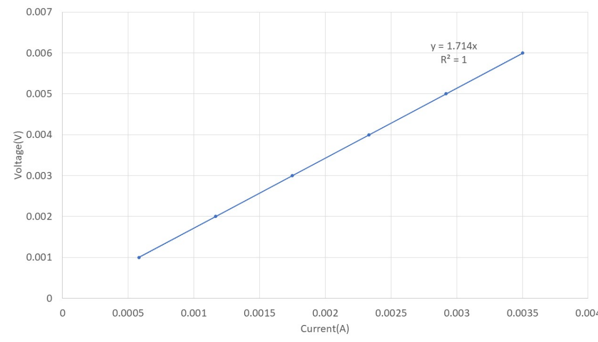

FIG. 7. Voltage vs Current curve for measuring probe resistance. The slope is the probe resistance

TABLE III. Raw data before annealing

Voltage(V)	Current(A)-1μm	Current(A)-2μm	Current(A)-2μm	Current(A)-6μm
0	0	0	0	0
0.01	0.000003	3.3E-06	0.000003798	4.52E-06
0.02	0.00000599	6.78E-06	0.000007266	8.03E-06
0.03	0.00000898	1.03E-05	0.00001074	1.15E-05
0.04	0.000012973	1.38E-05	0.000014225	1.5E-05
0.05	0.000016215	1.72E-05	0.000017701	1.86E-05
0.06	0.000019458	2.07E-05	0.000021178	2.21E-05
0.07	0.0000227	2.42E-05	0.000024656	2.56E-05
0.08	0.000025942	2.77E-05	0.000028132	2.91E-05
0.09	0.000029186	3.12E-05	0.00003161	3.26E-05
0.1	0.000032427	3.47E-05	0.000035086	3.61E-05

TABLE IV. Raw data after annealing

Voltage(V)	Current(A)-1μm	Current(A)-2μm	Current(A)-2μm	Current(A)-6μm
0	0	0	0	0
0.01	4.33E-06	0.000004427	4.41E-06	4.74E-06
0.02	8.7E-06	8.7352E-06	8.8E-06	9.46E-06
0.03	1.29E-05	0.000012947	1.32E-05	1.36E-05
0.04	1.71E-05	0.00001726	1.76E-05	1.8E-05
0.05	2.11E-05	0.000021632	2.2E-05	2.24E-05
0.06	2.52E-05	0.000025365	2.64E-05	2.7E-05
0.07	2.91E-05	0.000029375	3.08E-05	3.15E-05
0.08	3.31E-05	0.000033358	3.52E-05	3.55E-05
0.09	3.71E-05	0.000037284	3.96E-05	4E-05
0.1	4.11E-05	0.000041294	4.4E-05	4.48E-05

TABLE V. Voltage and current measurements for calculating probe resistance

Voltage(V)	Current(A)
0.001	0.000581
0.002	0.001166
0.003	0.001749
0.004	0.002333
0.005	0.002917
0.006	0.003502